RESEARCH ARTICLE

FUNCTIONALIZATION OF TEXTILE MEDICAL DEVICES FOR HERNIA REPAIR

*Emilia Visileanu, Laura Chiriac, Maria Memecică, Razvan Scarlat, Alina Vladu

The National Research and Development Institute for Textiles and Leather, 16, Lucretiu Patrascanu, street, 3rd District, Bucharest, Romania, cod 030508

ARTICLE INFO

ABSTRACT

Fabrication of biomaterials composed of natural and synthetic materials that are incorporated with an antibiotic is an attractive topic in wound healing. This study involves the design, development, and evaluation of a new multifunctional hernia mesh for the treatment of abdominal wall defects without complications. The developed hernia mesh is a composite of synthetic and natural materials with its backbone consisting of PES, PA and PP mesh to provide the required mechanical integrity. The meshes were coated with a natural, biodegradable, biocompatible and antimicrobial layer of chitosan (CS) for healing promotion and incorporating gentamicin sulfate (GS) as an antibacterial agent. The developed mesh showed excellent biocompatibility, antimicrobial activity and mechanical properties, and could be an ideal and feasible alternative mesh for hernia with many advantages, such as low cost, inertness, mechanical stability, pliability, low rate of infection, non-carcinogenicity, restricted inflammatory reaction, hypoallergenic and minimal complications.

Citation: Emilia Visileanu, Laura Chiriac, Maria Memecic , Razvan Scarlat, Alina Vladu. 2020. "Functionalization of textile medical devices for hernia repair", *International Journal of Current Research*, 12, (12), 14845-14853.

INTRODUCTION

Natural polymers offer the advantage of being similar to macromolecular substances, which the biological environment is prepared to recognize and to deal with metabolically. Problems associated with the stimulation of chronic inflammatory reaction and toxicity by synthetic polymers are largely suppressed or eliminated by using natural polymers. On the other hand, natural polymers are frequently quite immunogenic (Bano *et al.,* 2017). The purpose of this study was to prepare an optimal composite of materials as coating synthetic fibers like polyester, polyamide, and polypropylene for application in hernia surgery. The surface modification of the polyester fiber using NaOH is a topochemical reaction in which the hydroxyl ions of NaOH attack the carbonyl group of the PET fiber which forms disodium terephthalate and ethylene glycol. Due to their lower polarity, they may be responsible for providing easier access to the fiber surface, leading to a loss of mass of polyesters. Functionalization of fibers is a necessary condition for many industrial application processes, such as adhesion and coating which lead to an increase in fiber hydrophilicity. In the present study, we treated pes fabrics with a minimum amount of sodium hydroxide the surface leaching of PES fabric is a widely adopted process in the textile industry to achieve

smooth surface and increased hydrophilicity along with a reduction in the diameter and weight of the material. Polyester undergoes nucleophilic substitution and is hydrolyzed by aqueous sodium hydroxide. The hydroxyl ions attack the electron-deficient carbonyl of the polyester to form an intermediate anion. Chain scission follows and results in the production of hydroxyl and carboxylate end-groups: Attack occurs at fiber surfaces. The reaction of polyester with aqueous sodium hydroxide appears on the surface of the fibers, and thus it is topochemical. As chain scission occurs, the products of the reaction dissolve in the solution and reveal a fresh surface, which is attacked in turn. Functionalization of polyolefin surfaces is a prerequisite for many industrial application processes such as adhesion, coating, printing, etc. A densely functionalized polyolefin surface with preferably monotype functional groups is needed to graft molecules chemically for producing special surface properties. Functional groups such as OH are needed to form chemical bonds between inert polymer surfaces such as polyolefins to promote their adhesion to the desired coating. For their covalent bonding, the CHx groups of the macromolecule must be selectively substituted by OH radicals. This method involves the measurement of the wetting tension of a polypropylene film surface in contact with drops of distilled water in the presence of room temperature air. A contact angle of zero would indicate complete wetting. The angle increases as the surface become more nonpolar. Polycaprolactone (PCL) is an aliphatic polyester, widely used in (bio) medical applications due to its biocompatibility, moderate biodegradability, low cost, non-

Corresponding author: Emilia Visileanu,
The National Research and Development Institute for Textiles and Leather, 16, Lucretiu Patrascanu, street, 3rd District, Bucharest, Romania, cod 030508.

toxicity, and strong mechanical properties. However, PCL is hydrophobic which in some applications may severely limit the use of PCL. The blend of PCL with the natural chitosan polysaccharide, derived from chitin, could significantly improve its material characteristics (Goy, 2009; Younes, 2014). Chitosan actually provides hydrophilicity and antimicrobial activity, and further supports PCL's biocompatibility. To overcome these limitations, Chitosan has been mixed with synthetic biocompatible polymers such as polycaprolactone (PCL) and an antibiotic, gentamicin sulfate. PCL is an FDA approved biocompatible material with optimum mechanical and degradation properties suitable for medical applications (Kong, 2010).

The morphological analysis of the samples was performed by Scanning Electron Microscopy and it can be observed that the fibers are partially coated. Blending hydrophilic chitosan with hydrophobic PCL is an attractive option due to its flexibility in combining with other polymers facilitated by its low melting point (60 °C). It is a biodegradable and biocompatible polyester with excellent tensile properties (Loïc, 2016). The amine group of chitosan could potentially form an amide bond with the carbonyl group of ester groups in the chain or carboxylic acid groups at the end of chains of PCL (Okamoto, 2003). Graft copolymers CS-g-PCl can be prepared by linkage of PCL to either free hydroxyl or free amino groups on the chitosan backbone (Busilacchi *et al., 2013*).

MATERIALS AND METHODS

Materials: Chemicals used were purchased from Sigma-Aldrich. PCL (Mn = 80 000), PCL (Mn~530), chitosan (medium molecular weight, degree of deacetylation 75–85% according to 1 H-NMR), Gentamicin Sulfate (40 mg/mL), Acetic Acid, Ethanol, Hydrogen Peroxide, Sodium Hydroxide. Pre-treatment for improving the wettability of PP and PA fibers was made by using the process and chemicals/parameters presented in Table 1.

Table 1. Fibers pre-treatment

Textile fiber	Process	Chemicals/ parameters
Polypropylene	Oxidative treatment Rinsing	10% H_2O_2, 2H, 25
Polyamide	Oxidative treatment Rinsing	10% H_2O_2, 2H, 25
Polyamide	Alkaline treatment Neutralization Rinsing	2% NaOH, 2H, 25
Polyamide	Oxidative treatment Alkaline treatment Neutralization Rinsing	10% H_2O_2, 2% NaOH, 2H, 25

Synthesis of CS-Graft-PCL: Chitosan solutions of different concentrations were prepared by dispersing chitosan powder into deionized water, followed by addition under stirring of diluted acetic acid to dissolve chitosan at room temperature under magnetic stirring (300 rpm) for 4H. Recipes were applied on polypropylene, polyamide and polyester knitted meshes (Table 2).

Table 2. Recipes used for surfaces treatment

No.	Recipe	Treatment Method
1	0,4 % Chitosan (w/v)	Exhaustion
2	0,8 % Chitosan (w/v)	Padding
3	1:1 volume ratio Chitosan-PCL	Padding

Determination of chitosan content on samples: The samples to be extracted are placed in a glass extraction cartridge in such a way as to avoid material loss. The sample cartridge is inserted into the extraction apparatus, Soxhlet, to the edge of the siphon. The solvent is introduced into the extraction flasks in sufficient quantity to ensure the first siphoning. Set the silicone oil bath to 100 ℃. The extraction is considered complete after approximately 12 siphons. Remove the sample cartridges, squeeze with tweezers, leave to dry, then place in the weighing ampoules and dry at 105 °C, cool in the desiccator for 30 minutes, and weigh.

The results were calculated by formula 1.

$$B C = m_2 / m_1 \cdot 100 \ (\%) \tag{1}$$

where: m_1 is mass of the sample (g); m_2– the mass of extract (g).

RESULTS AND DISCUSSION

In the table 3 is presented the loading degree of the textile structures treated with 0,8% chitosan. The best value of 1,28% was obtained for the textile structure made of 100% polyamide, followed by the one from polypropylene (1,01%) and the one from polyester (0,98%).

Table 3. Chitosan content

No.	Sample Code	Extract Weight (mg)	Percentage from initial sample mass (%)
1	V19PA – CC	1,06	1,28
2	V21PP – CC	0,22	1,01
3	V20PES – CC	0,094	0,98

Young's modulus

The elongation-effort curves were determined for the untreated mesh variants (table 4) and Young's modulus was calculated according to the formula 2.

Young's modulus according to Hooke's law:

$$E = \frac{\sigma}{\varepsilon} = \frac{F \cdot L_0}{A \cdot \Delta L} \tag{2}$$

where:

E is Young's modulus (MPa);

σ– uniaxial stress or uniaxial force per unit area (N/m2);
ε– strain is the deformation or proportional deformation (change in length divided by the initial length); dimensionless

F – applied force (N);
A – cross-sectional surface area (m^2);
L – change in length (m);
L_0 – initial length (m).

In the table 5 are presented the main calculation parameters of Young's modulus and the values of Young's modulus obtained for the variants of untreated textile structures. From the analysis of the data presented in table 1 and table 2 results the following aspects regarding the modulus of elasticity of untreated textile structures:

Table 4. Effort-elongation curves of untreated meshes

No.	Variant	Effort-elongation curves of untreated meshes	
		Warp	Weft
1	V19-PA		
2	V20PES		
3	V21PP		
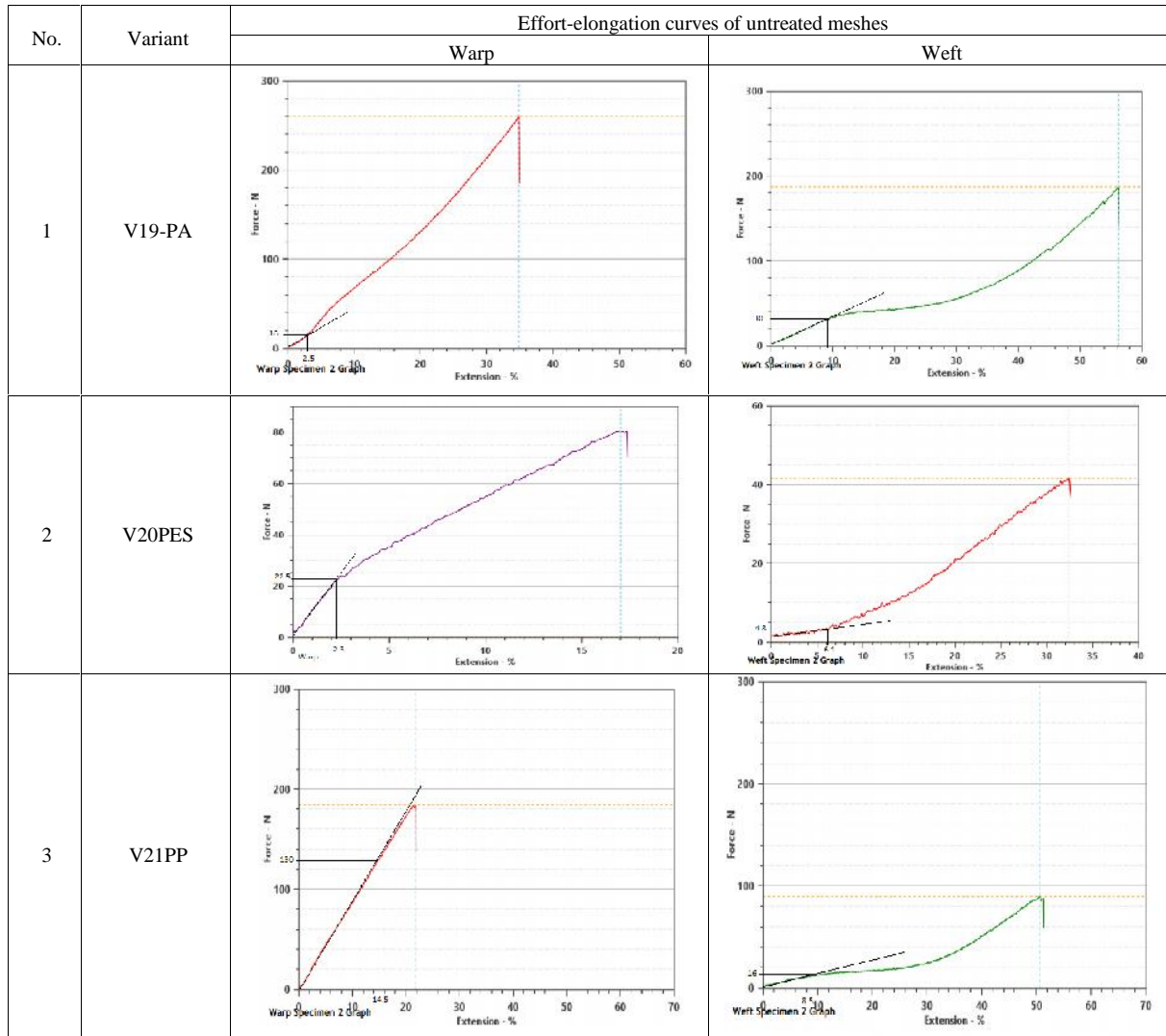
Table 5. Young's Modulus values

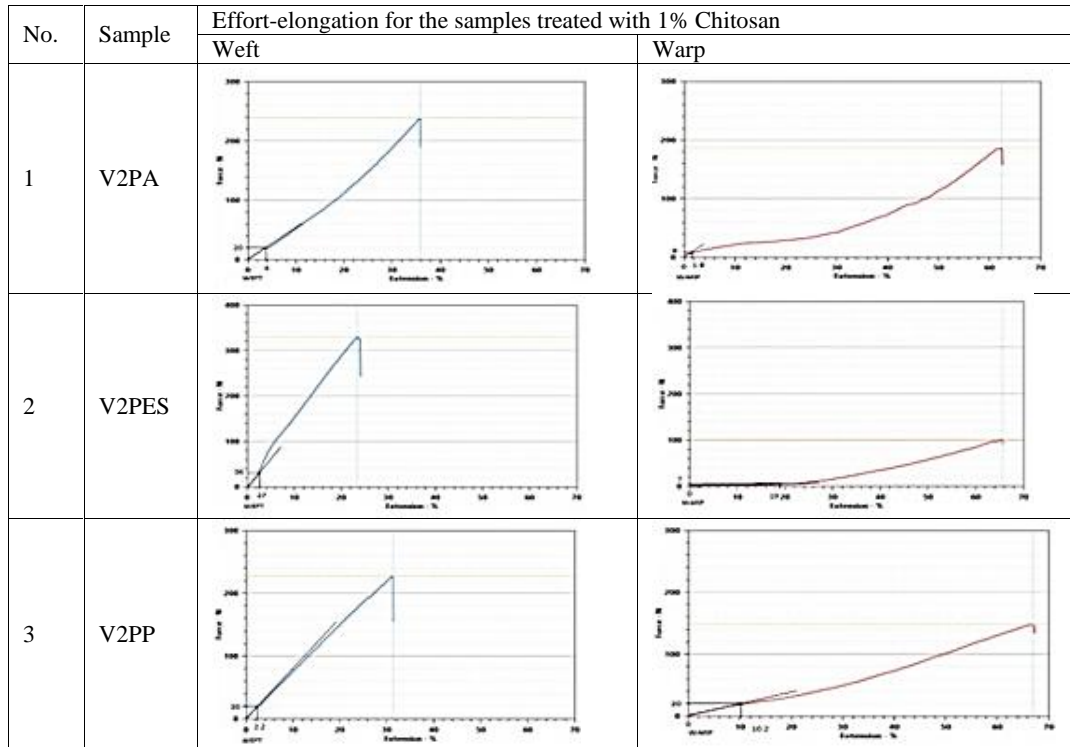| No.	Sample	Parameters						Elasticity	
		Force (N)	L_0 (cm)	L_1 (cm)	L (cm)	A (cm^2)	G (mm)	(N/cm^2)	(MPa)
1	V20 weft	4.72	5	5.326	0.32	0.23	0.46	314.75	3.15
	V20 warp	19.9	20	20.46	0.46	0.92	0.46	940.45	9.40
2	V19 weft	35	5	5.535	0.53	0.3	0.6	1090.34	10.90
	V19 warp	17	20	20.76	0.76	1.2	0.6	372.81	3.73
3	V21 weft	16.5	5	5.5125	0.51	0.32	0.64	503.05	5.03
	V21 warp	136	20	22.95	2.95	1.28	0.64	720.34	7.20

⌡ The textile structures that are located with Young's modulus, in both directions, at the level of the value specific to the abdominal fascia (approx. 11 MPa) are: V19 PA (10.9 MPa and 3.73 MPa respectively), V20PA (3.15 MPa and 9.40 MPa respectively), V21PP (5.03 MPa and 7.20MPa;

⌡ These composite structures with a lower Young's modulus in both directions (V19PA, V20PES, V21PP) do not generate high shear forces but have a higher degree of deformation. In general, because the abdominal wall behaves almost twice as elastic vertically compared to horizontal, meshes with higher elasticity are needed in the craniocaudal direction for the midline of the defect repair area. In vivo studies can define the best anisotropic mesh location.

⌡ The V15PES textile structure obtained from multifilamentary PES presents on the vertical direction, a higher value of Young's modulus (33.69MPa) as compared to the specific value of the abdominal fascia.

Composite structures with a high elastic modulus (V15 PES) in one direction, or both directions, generally have a low elongation value providing strong mechanical reinforcement of the abdominal wall, but at the cost of increasing shear forces between the mesh and the abdominal wall. Increased shear forces have been shown to contribute to chronic local trauma, leading to fibrotic growth/remodeling and subsequent low quality of patient life. In table 6 the effort-elongation curves are presented for the samples treated with 1% Chitosan.

Table 6. The effort-elongation curves for the samples treated with 1% Chitosan

No.	Sample	Effort-elongation for the samples treated with 1% Chitosan	
		Weft	Warp
1	V2PA		
2	V2PES		
3	V2PP		

Table 7. Young's modulus for the samples treated with Chitosan

No.	Variant	Parameters						Elasticity	
		Force (N)	L_0 (cm)	L_1 (cm)	L (cm)	A (cm^2)	G (cm)	(N/cm^2)	(MPa)
1	V2PA weft	20	5	5.2	0.2	0.35	0.071	1408.45	14.08
	V2PA warp	9	20	20.36	0.36	1.42	0.071	352.11	3.52
2	V2PES weft	36	5	5.135	0.135	0.08	0.016	8333,2	88,3
	V2PES warp	7	20	23.8	3.8	0.32	0.016	1151.32	11.51
3	V2PP weft	20	5	5.11	0.11	0.21	0.042	4329	43.29
	V2PP warp	20	20	22.04	2.04	0.84	0.042	233.43	2.33

Table 8. The effort-elongation curves for the samples treated with Chitosan+PCL

No.	Sample	Effort-elongation curves for the samples treated with Chitosan+PCL	
		Weft	Warp
1	V19CC		
2	V20CC		
3	V21CC		
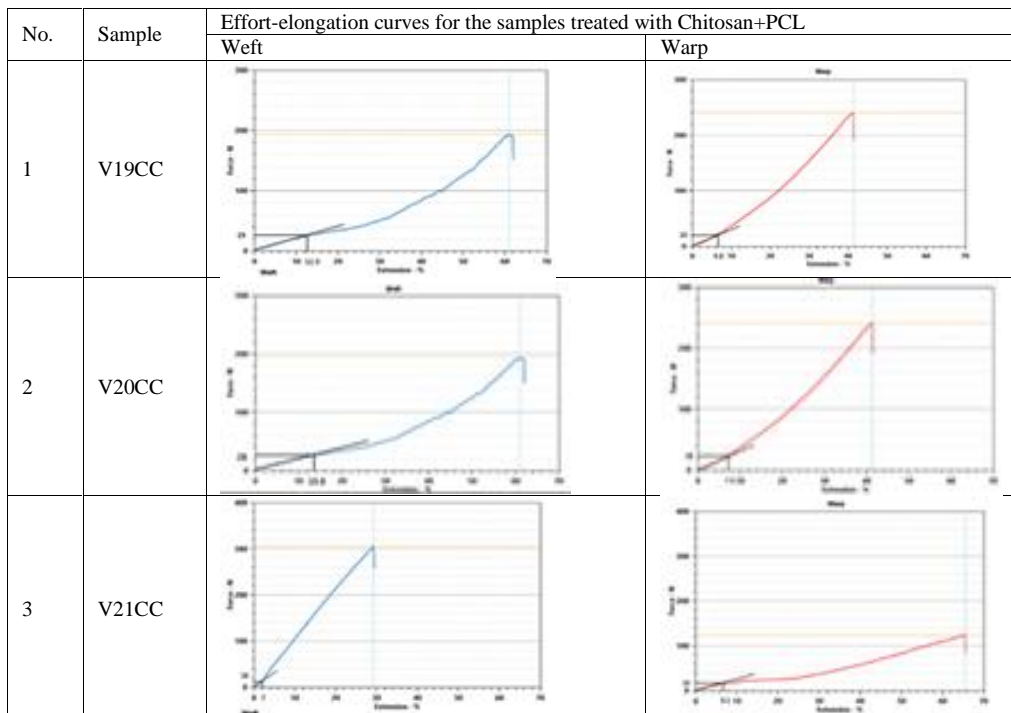
Table 9. Young's modulus for the samples treated with Chitosan+PLC

No.	Variant	Parameters							
		Force (N)	L_0 (cm)	L_1 (cm)	L (cm)	A (cm^2)	G (cm)	Young's modulus (N/cm^2)	(MPa)
1	V19PACC weft	25	5	5.615	0.615	0.365	0.073	556.85	5.57
	V19PA CC warp	20	20	21.36	1.36	1.46	0.073	201.45	2.01
2	V20PES CC weft	28	5	5.69	0.69	0.085	0.017	2387.04	23.87
	V20PES CC warp	26	20	21.46	1.46	0.34	0.017	1047.54	10.48
3	V21PP CC weft	16	5	5.1	0.1	0.195	0.039	4102.56	41.03
	V21PP CC warp	19	20	21.24	1.24	0.78	0.039	392.89	3.93
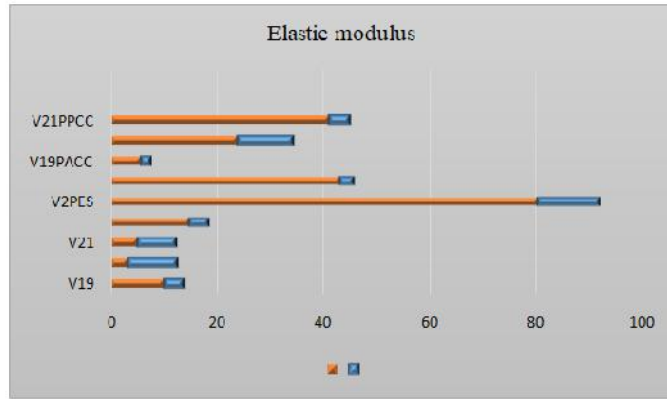
Fig. 1. Evolution of Young's modulus

Table 10. Young's Modulus and Anisotropy for untreated and treated samples with Chitosan and Chitosan+PCL

No.	Sample	Parameters		
			Young's Modulus (MPa)	Anisotropy
1	V20	weft	3,15	0,475
		warp	9,4	
2	V19	weft	10,9	0,466
		warp	3,73	
3	V21	weft	5,03	0,156
		warp	7,2	
4	V2PES	weft	166,6	1,160
		warp	11,5	
5	V2PA	weft	14,08	0,602
		warp	3,52	
6	V2PP	weft	43,2	1,269
		warp	2,33	
7	V20PES-CC	weft	23,8	0,357
		warp	10,4	
8	V19PCC	weft	5,57	0,443
		warp	2,01	
9	V21PP-CC	weft	41,03	1,019
		warp	3,93	
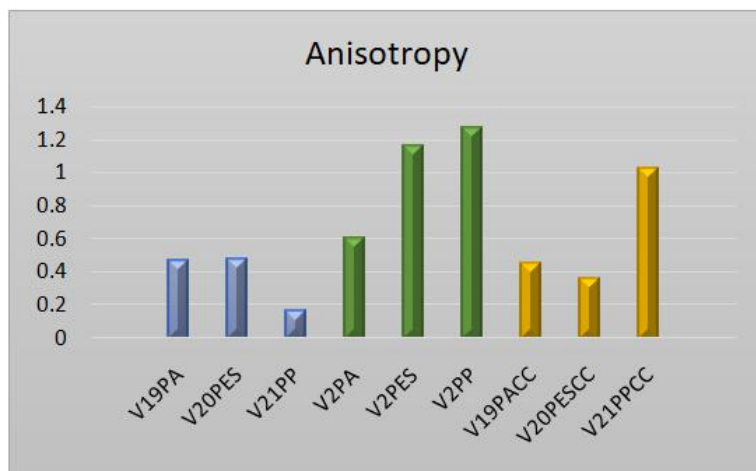
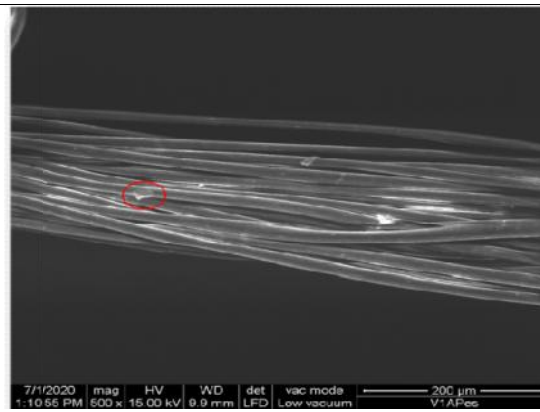

Fig. 2. Anisotropy evolution

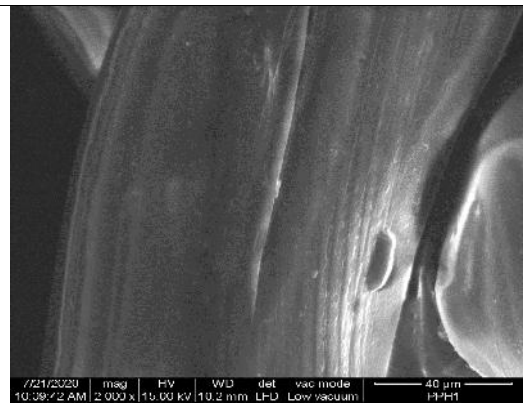**Fig. 3. SEM images of PES yarns after treatment**

Fig. 4. SEM images of PP yarns after treatment
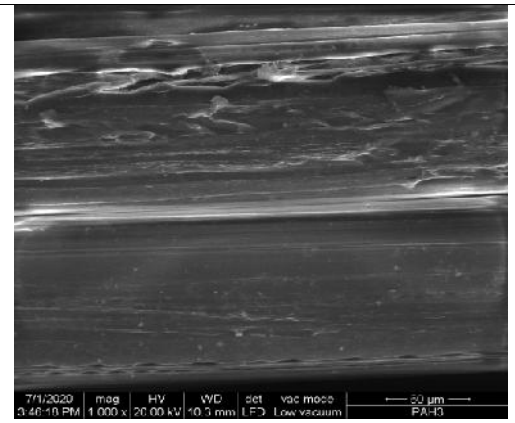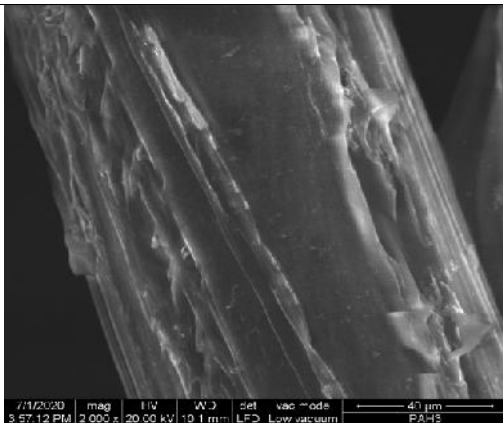

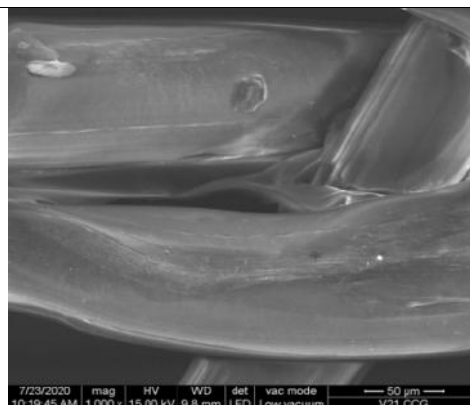**Fig. 5. SEM images of PA yarns after treatment**

**Fig. 6. SEM image of polypropylene yarns coated
with PCL-Chitosan-Gentamicin sulfate**

Table 11. Contact angle after PA treatment

Initial		After surface modification					
Polyamide		**PAH1**		**PAH3**		**PAH4**	
Left	Right	Left	Right	Left	Right	Left	Right
106,73°	107,13°	Hydrophile		Hydrophile		96,30°	97,26°
		Contact angle = 0		Contact angle = 0			

Table 12. Contact angle after PP

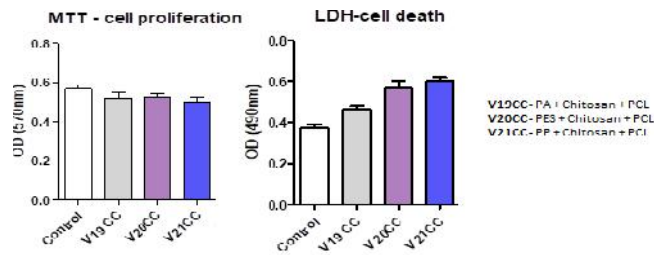| Initial		After surface modification	
Polypropylene			
Left	Right	Left	Right
128,40°	121,16°	121,16°	120,40°

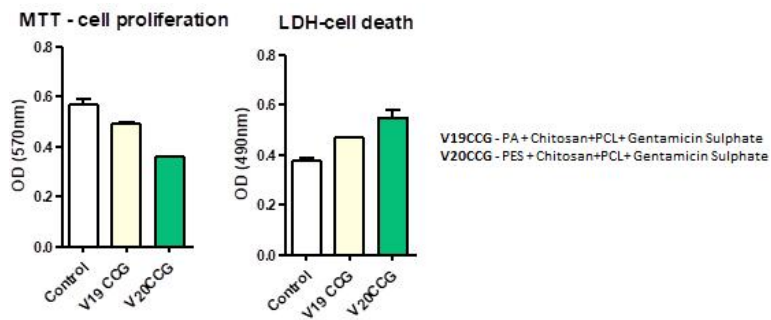**Fig.7. MTT and LDH values-chitosan treatment**

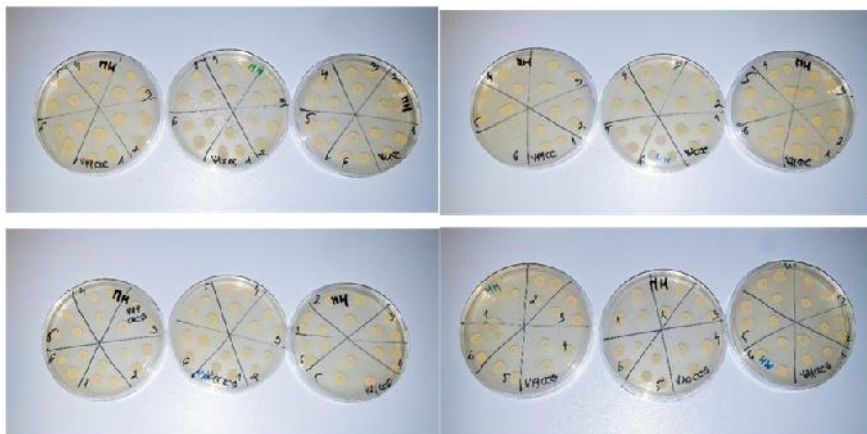**Fig.8. MTT and LDH-chitosan and gentamicinatretment**

Fig. 9. Antimocrobial activity

Table 7 presents the main calculation parameters of Young's modulus and the values of the elastic modulus obtained for the textile structures treated with chitosan. From the analysis of the data presented in table 7 the following can be observed:

- All variants of textile structures treated with chitosan have higher values of Young's modulus compared to untreated samples, in at least one of the directions (figure 1);
- All variants of textile structures treated with chitosan have higher values of Young's modulus, in at least one direction, as compared to the specific value of the abdominal fascia of 10.9 MPa.

In table 8 the effort-elongation curves are presented for the samples treated with chitosan 1% Chitosan and 1% PLC and in table 9 are presented the main calculation parameters of the elastic modulus and the values of the elastic modulus for the textile structures treated with chitosan + PLC. From the analysis of the data presented in table 9, for the samples treated with chitosan + PLC the following can be observed:

The variant with Young's modulus <10.7MPa, specific to the abdominal fascia is V19PACC – of 100% PA (weft –5.57MPa and Warp –2.01MPa); modulus of elasticity has lower values, in this variant compared to the untreated variant (weft: 5.57 compared to 10.9 and warp: 2.01 compared to 3.73. The textile structures with Young's modulus higher in at least one direction compared to the specific value of the abdominal fascia are V20PES-CC and V21PA-CC; these structures also present, at least in one of the directions, higher values of the elasticity, compared to the untreated samples (figure 1). All variants have a higher Young's modulus in the transverse direction compared to the horizontal direction (90.1% – V21PP-CC and 52% –V20PES-CC); Composite structures with a high elastic modulus (V20PES-CC and V21PP-CC) in a certain direction, or in both directions, generally have a low elongation value providing a strong mechanical reinforcement of the abdominal wall, but at the cost of increasing the forces of shear between the mesh and the abdominal wall. Increased shear forces have been shown to contribute to chronic local trauma, leading to fibrotic growth/remodeling and subsequent low quality of patient life. In figure 1 is illustrated the evolution of the values of Young's modulus for the untreated samples, treated with chitosan and chitosan PLC.

Anisotropy

Mesh anisotropy is an important characteristic with potential implications for the abdominal wall. By definition, the mechanical behavior of an anisotropic network in one direction is different from its behavior in another direction. As a result, the orientation of an anisotropic implant has an important impact on the mechanical behavior of the repaired abdominal wall. Anisotropy is formulated as the ratio between the elastic modulus of the horizontal and vertical axes, according to the relation:

$$K = \left| l\epsilon \quad \frac{E_w}{E_w} \right| \tag{3}$$

In table 10 the values of anisotropy are presented for the variants of textile structures untreated and treated with Chitosan and Chitosan + PCL.

From the analysis of the data presented in table 10 and figure 2 the following aspects can be ascertained:

- the best values of anisotropy are recorded for the variants of textile structures from 100% PA treated with chitosan (0.602) and chitosan + PLA (0.443), these values are at the level of variants from 100% PA-untreated;
- the V20PES-CC variant has a good anisotropy value (0.357), lower than the untreated sample (0.475); the V2PES variant has a higher anisotropy value (1,160) compared to the untreated sample (0.475);
- 100% PP textile structures have high anisotropies (V2PP – 1,209 and V21PP-CC –1,019); these values exceed about 10 times the value recorded for untreated samples (0.156);
- In all cases the anisotropy of the variants of textile structures treated with chitosan + PCL is lower compared to those treated only with chitosan.

Scanning Electron Microscopy: Scanning Electron Microscopy (SEM) images are usually used to show the morphology of polymer blends. For PES and PP fibers attack occurs at the surface after treatment and this is supported by SEM images as is shown in figure 1, and figure 2. Scanning Electron Microscopy demonstrated that the polyamide surface had been physically altered and the contour changed in figure 3. Images of Chitosan-PCL composite containing gentamicin sulfate are shown in figure 4. In the images it can see small white spots on the surface of the fibers; this proves that gentamicin was adsorbed on the sample's surface. Moreover, from SEM images it can see that the films are homogenous.

Contact angles measurements

This method involves the measurement of the wetting tension of meshes surfaces in contact with drops of distilled water in the presence of room temperature. A contact angle of zero would indicate complete wetting (PAH1, PAH3). The angle increases as the surface become more non-polar. A drop is held at equilibrium by three interfacial tensions: solid-air (tensile pulling to the right), liquid-air (tensile pulling in the direction), and solid-liquid (tensile pulling to the left). Contact angle measurements that interact directly with the surface did show significant surface differences. The surface became more polar (table 11and table 12).

Biocompatibility assessment: Biocompatibility was analyzed using the MTT and LDH tests MTT assay is a quantitative test that allows evaluation of both cell viability and proliferation. Briefly, HT-29 epithelial cells were incubated with 1 mg/ml (3-(4.5-dimethylthiazol-2yl))-2.5-diphenyltetrazolium bromide (MTT) solution for 4 h in the dark, at 37ºC. Formazan crystals were solubilized with HCl-SDS, resulting in a purple solution, quantified by spectrophotometry at 570 nm, using FlexStation3 (Molecular Devices, USA). The LDH test (Tox7 kit, Sigma-Aldrich) was performed according to the manufacturer's instructions. Cells that no longer have membrane integrity release lactate dehydrogenase (LDH) into the culture medium. The culture medium was collected and mixed with the kit's components to be evaluated 4 days of culture by spectrophotometric readings at 490 nm. For qualitative analysis of biocompatibility, cells were stained with fluorescein diacetate (FDA) and cell morphology was analyzed by microscopy (Carl Zeiss AxioScope, Jena, Germany) and

then processed with Zeiss Zen 2010 software. Statistical analysis was performed using Graph Pad Prism 6.0 software, Unpaired t-test. Statistically significant values were considered for $p<0.05$. Out of the tested variants, V19 CC had the highest biocompatibility, with high MTT and low LDH values (figure 7). Out of the variants with gentamicin sulfate, V21CCG are bored the highest biocompatibility when tested on HT-29 epithelial cells (figure 8).

Antimicrobial Activity: The obtained results indicate no antimicrobial activity. Growth can be observed on all dilutions inoculated (figure 9). No logarithmic reduction.

Conclusions

In this study, it has been shown that by oxidative treatment and alkaline hydrolysis of PA, PP, PES meshes, hydrophilicity increased according to the contact angles. After increasing the hydrophilicity, the textile structures V19PA, V21PP, and V20PES were treated with chitosan, and according to the results provided by the degree of loading all samples were adsorbed approximately 1% chitosan. All variants of untreated textile structures show the modulus of elasticity at the level of the abdominal fascia (<10MPa); among the treated variants, the textile structure variant made of 100% PA treated with chitosan and PLC falls at this level. All variants of untreated textile structures show anisotropy at the level of the abdominal fascia (<1.0); among the treated variants are at this level: V2PA (treatment with chitosan), V19PACC, and V20PESCC (treated with chitosan and PLC). According to the MTT and LDH results, V19PACC and V19PAvCCG had the best biocompatibility. Chitosan coated polypropylene mesh can act as an antiadhesive barrier when used in the repair of incisional hernias and abdominal wall defects. Moreover, the chitosan and gentamicin sulfate coated meshes demonstrated excellent antimicrobial release properties. Thus, a bio-based chitosan mesh with suitable antimicrobial properties could be used for infection prevention during hernia repair.

REFERENCES

Bano, I., Arshad, M., Yasin, T., Ghauri, M.A., Younus, M., *Chitosan: A potential biopolymer for wound management*, In: International Journal of Biological Macromolecules, 102: p. 380–383, 2017.

Busilacchi, A., Gigante, A., Mattioli-Belmonte, M., Manzotti, S., Muzzarelli, R.A.A. *Chitosan stabilizes platelet growth factors and modulates stem cell differentiation toward tissue regeneration*. In: Carbohydr. Polym. 2013, 98, 665–676.

Goy, R.C., Britto, D.D., Assis Oiii, B.G. *A review of the antimicrobial activity of chitosan*. In: Polímeros 2009, 19, 241–247.

Kong, M., Chen, X.G., Xing, K., Park, H.J. *Antimicrobial properties of chitosan and mode of action: A state of the art review*. In: Int. J. Food Microbiol. 2010, 144, 51–63.

Loïc, B., Catherine, L. *Interests of chitosan nanoparticles ionically cross-linked with tripolyphosphate for biomedical applications*. In: Prog. Polym. Sci. 2016, 60, 1–17.

Okamoto, Y., Yano, R., Miyatake, K., Tomohiro, I., Shigemasa, Y., Minami, S. *Effects of chitin and chitosan on blood coagulation*. In: Carbohydr. Polym. 2003, 53, 337–342.

Younes, I., Sellimi, S., Rinaudo, M., Jellouli, K., Nasri, M. *Influence of acetylation degree and molecular weight of homogeneous chitosan on antibacterial and antifungal activities*. In: Int. J. Food Microbiol. 2014, 185, 57–63.

****